UNIVERSITY OF CAMBRIDGE
Department of Engineering

Fourth Year Project Report

Relay Feedback Models of Biological Oscillators

Rajiv Kurien

Queens' College

2015-2016

Supervisor: Prof.R.Sepulchre

I hereby declare, that except where specifically indicated, the work submitted herein is my own original work.

Signed _____ Date: 24 May 2016

Technical Abstract

Biological behaviours are complex, rich and varied. Oscillations in biology are diverse and models replicating them are often high dimensional and nonlinear. These models quickly get difficult to analyse and do not have a generalised theory (except for in two dimensional systems) to predict the existence of oscillations, their stability and their time periods. However, the theory of relay feedback systems, a very particular type of nonlinear feedback, used classically in automatic control, has analytical solutions to these questions.

The aim of this project was to elucidate how useful the theory of relay feedback systems would be to analysing biological oscillations. As a first step, the basic model of relay feedback was applied to two classical biological models — the Goodwin oscillator model for genetic oscillations and the FitzHugh-Nagumo model for action potentials. Relay feedback was able to simulate oscillations in these models, reflecting upon how biological oscillations often incorporate digital and analogue dynamics.

As a second step, the potential of nested relay feedback to model complex oscillations was investigated. A normal form model of neuronal bursting was dissected as two interconnected relay feedback systems. The Hindmarsh-Rose model of neuronal bursting was then shown to have the same structure as the normal form model, conceding it to be modelled by relay feedback.

The project revealed how relay feedback provides an appealing modelling framework for the analysis of quantitative models of biological oscillations. It highlights how biological models can be viewed as an interconnection of analogue (L.T.I) and digitial (relay) logic. Due to the theory of relay feedback oscillations being tractable in high dimensions, it provides a way of analysing high order biological models and is amenable to robustness and sensitivity analysis.

Contents

1 Introduction

Oscillations are an integral component in the world around us. Biochemical and biophysical rhythms are ubiquitous characteristics of living organisms, from rapid oscillations of membrane potential in nerve cells to slow cycles of ovulation in mammals [1]. Understanding the molecular and cellular mechanisms responsible for oscillations is crucial for unravelling the dynamics of life [2]. Fundamentally, oscillations are due to feedback, and classical control has usually been applied to reduce these oscillations. With the pursuit of understanding biological oscillations, feedback models have been explored to understand how to generate different types of oscillations. Such research aims to yield a better understanding of how biology works, giving us tools to engineer biology to suit our needs.

Several models of biological oscillations display logic. Gene regulatory models incorporate a gene turning on or off. Neuronal models are excitatory, displaying oscillations when a threshold is exceeded. Such biological models of oscillations inherently combine analogue and digital signals. They may have a large number of parameters that require tuning in order to produce oscillations and pose difficulties in extracting useful information about the effect of these parameters on existence of oscillations and their frequency. Figure 1 shows how for a particular three variable dynamical system, changing two parameters reveals a rich repertoire of oscillatory behaviours. A method of addressing models of oscillations described in [2], simply amounts to simulating the system around the parameter space that is available or in a physiological range. For high dimensional systems, a parameter search approach is computationally expensive.

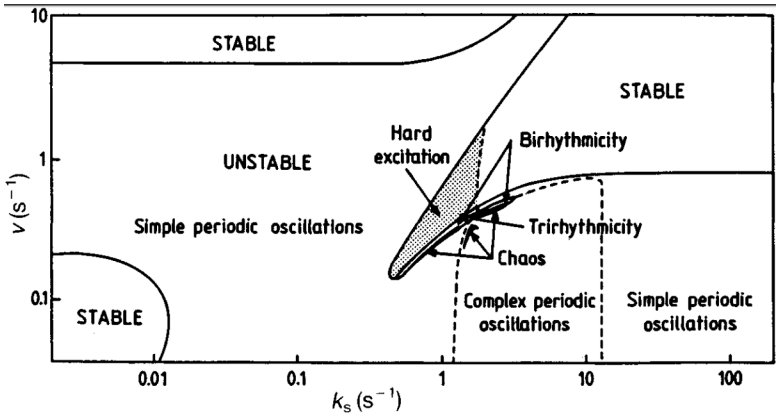

Figure 1: Different domains of dynamic behaviour in the parameter space $v - k_s$ for a three variable multiply regulated biochemical system. Source [3].

Another method of tackling this issue is to model oscillations as adaptation around a static nonlinearity. This approach links biological oscillation to a methodology developed in classical control — relay feedback systems, which gives us tools to analyse oscillations.

Relay feedback consists of a plant connected via negative feedback to a static hysteretic nonlinearity called a relay. Relay feedback is most popularly used in automatic tuning of PID controllers. It is one of the simplest and most robust auto-tuning techniques for process controllers and has been successfully applied to industry for more than 15 years [4]. Oscillations in simple relay feedback systems have

been well understood and have analytical results even for high dimensional systems.

Consequently, this raises the question: Are relay feedback models appropriate to analyse biological oscillations?

This project starts to address this question, and the report is structured as follows. In section 2, some of the analytical results for oscillations in relay feedback systems from [5] are presented. Section 3 uses a simple relay feedback system to model continuous oscillations in the Goodwin and FitzHugh-Nagumo models. Finally, section 4 investigates using two coupled relay feedback systems to model a complex oscillation — bursting, and consequently the famous Hindmarsh-Rose model for neuronal bursting.

2 Theory

A relay is a particular type of nonlinearity that has only two output values, a high or a low value, dependent on the input. Figure 2 shows a symmetric relay element that satisfies the input (e) and output (u) relationship:

$$u(t) = \begin{cases} d \text{ if } e > \epsilon \text{ or } (e > -\epsilon \text{ and } u(t-) = d) \\ -d \text{ if } e < -\epsilon \text{ or } (e < \epsilon \text{ and } u(t-) = -d) \end{cases} \tag{1}$$

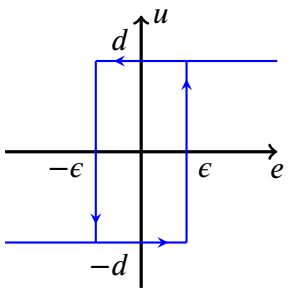

Figure 2: Relay element

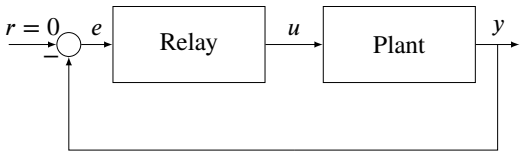

Figure 3: Relay feedback

Figure 3 reveals how a typical relay feedback system is connected. The output of a plant (y), is connected to the relay ($e = -y$), and the output of the relay is input to the plant. Relay feedback systems tend to cause oscillations as the plant is subjected to maximal input (high or low) in the opposite direction when the plant exceeds a threshold (ϵ or $-\epsilon$), as shown in Figure 4.

Relay feedback systems combine analogue and digital signals, which is reminiscent of switching behaviour in biological oscillations.

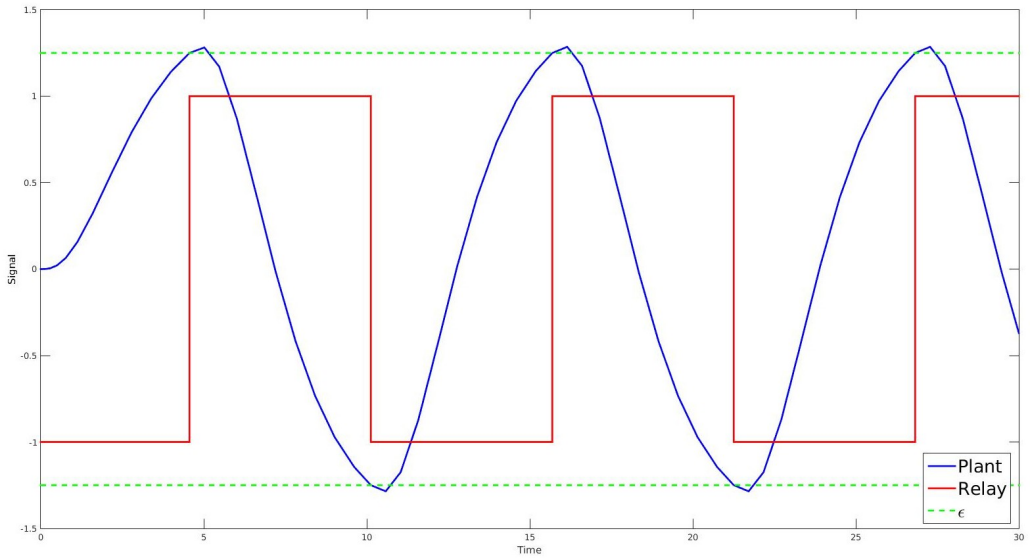

Figure 4: Oscillations in a relay feedback system. The relay switches when the plant reaches the hysteresis limits $\pm\epsilon$, causing the plant to oscillate between those limits.

2.1 Symmetric oscillations

Consider the linear time invariant system:

$$\begin{aligned} \dot{x} &= Ax + Bu \\ y &= Cx \end{aligned} \tag{2}$$

When this system is connected to the relay (1), with $e = -y$, the system can have a symmetric limit cycle of period $T = 2h$ if the following condition is met:

$$C(I + e^{Ah})^{-1} \int_0^h e^{As} B \mathrm{d}s = \frac{\epsilon}{d} \tag{3}$$

This theorem is able to deal with high dimensional systems, giving a general approach to analysing nonlinear models of oscillations.

2.2 Asymmetric oscillations

When the relay is characterized by:

$$u(t) = \begin{cases} d_1 \text{ if } e > \epsilon \text{ or } (e > -\epsilon \text{ and } u(t-) = d_1) \\ -d_2 \text{ if } e < -\epsilon \text{ or } (e < \epsilon \text{ and } u(t-) = -d_2) \end{cases} \tag{4}$$

The LTI system given by (2) can have asymmetric oscillations when $e = -y$ and the following conditions for a limit cycle with period T are met:

$$\begin{cases} C(I - \Phi)^{-1}(\Phi_2 \Gamma_1 d_1 - \Gamma_2 d_2) = -\epsilon \\ C(I - \Phi)^{-1}(-\Phi_1 \Gamma_2 d_2 + \Gamma_1 d_1) = \epsilon \end{cases} \tag{5}$$

where

$$\Phi = e^{AT}\ ,\ \Phi_1 = e^{A\tau}\ ,\ \Phi_2 = e^{A(T-\tau)}$$
$$\Gamma_1 = \int_0^{\tau} e^{As}\mathrm{d}s\boldsymbol{B}\ ,\ \Gamma_2 = \int_0^{T-\tau} e^{As}\mathrm{d}s\boldsymbol{B} \tag{6}$$

The asymmetric oscillation is split into two parts, a period when the relay output is low, τ, and the period when the relay output is high, $T - \tau$, as shown in Figure 5.

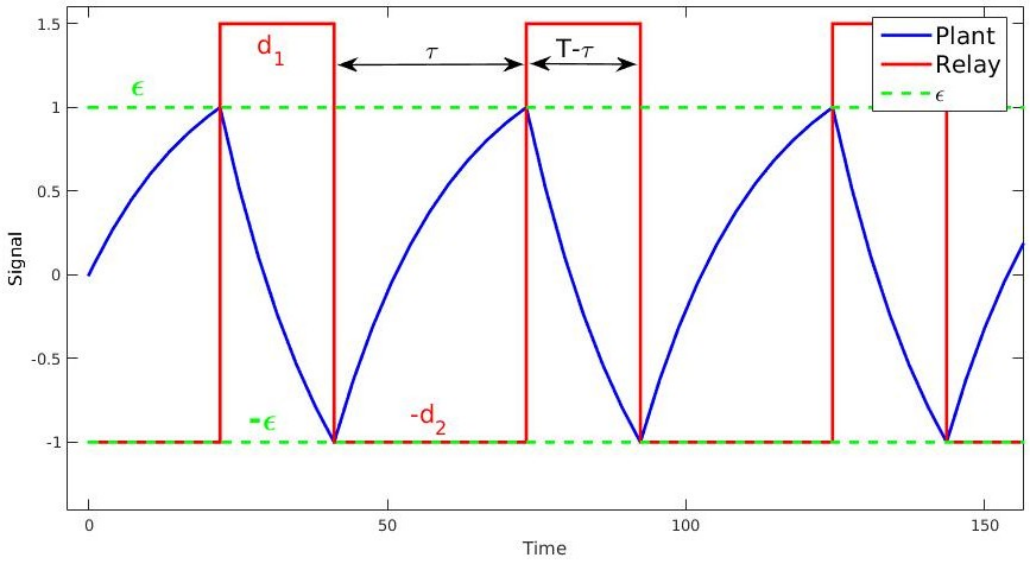

Figure 5: Asymmetric oscillations with relay feedback.

In this project, once a model was approximated using relay feedback, the tools stated above were used to predict the existence of limit cycles and their time periods. Parameters of a model could be varied and their effect understood by the above equations. [5] also derived initial conditions for these oscillations and how to check the local stability of the oscillations, which again were used to analyse each model.

3 Relay feedback models of fundamental biological limit cycles

Two fundamental models of continuous oscillations in biology will be modelled as simple relay feedback systems in this section. This proof of concept step reveals the use of relay feedback in order to predict time periods of oscillations and understanding how different parameters affect oscillations.

3.1 Goodwin oscillator model

The Goodwin oscillator is a biochemical oscillator model based on negative feedback alone. This genetic oscillator describes the conceptual mechanism of how mRNA, protein and end product interact.

Written in their non-dimensional form [1], the Goodwin oscillator's kinetic equations are:

$$\frac{dx_1}{dt'} = \frac{1}{1+x_3^p} - b_1 x_1 \tag{7}$$

$$\frac{dx_2}{dt'} = b_2(x_1 - x_2) \tag{8}$$

$$\frac{dx_3}{dt'} = b_3(x_2 - x_3) \tag{9}$$

where $x_1, x_2.x_3$ are non-dimensionalised concentrations of mRNA, protein and end product, respectively. The only nonlinearity, $(\frac{1}{1+x_3^p})$, becomes a relay with no hysteresis as $p \to \infty$ (see Figure 6).

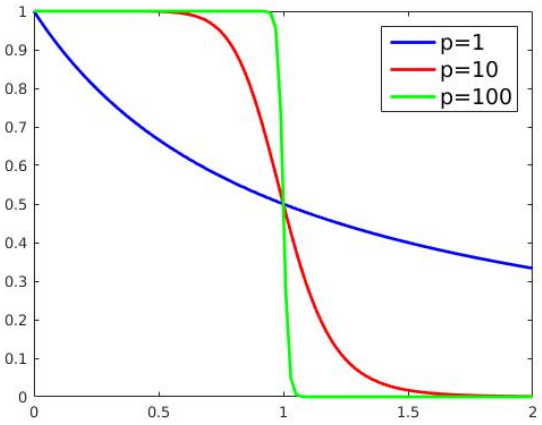

Figure 6: Nonlinearity becomes a relay with no hysteresis, as $p \to \infty$.

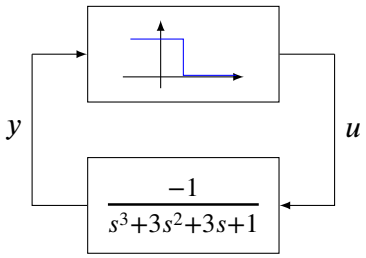

Figure 7: Relay feedback system model of Goodwin oscillator ($b_1 = b_2 = b_3 = 1$).

Setting $b_1 = b_2 = b_3 = 1$ (for simplicity) and rewriting the equations such that the linear equations form the plant and the nonlinearity is a relay, results in the system shown in Figure 7 with the state space realisation:

$$\dot{x} = \begin{bmatrix} -1 & 0 & 0 \\ 1 & -1 & 0 \\ 0 & 1 & -1 \end{bmatrix} x + \begin{bmatrix} 1 \\ 0 \\ 0 \end{bmatrix} u \tag{10}$$

$$y = \begin{bmatrix} 0 & 0 & 1 \end{bmatrix} u \tag{11}$$

$$u = \begin{cases} 0 \text{ if } e \geq 1) \\ 1 \text{ if } e < 1) \end{cases} \tag{12}$$

Using the theory for asymmetric oscillations, initial conditions were derived numerically. The limit cycle with the appropriate time period was shown to be locally stable and the simulations of the Goodwin model (with a large p) and the relay feedback model were very similar (see Figure 8). This (novel) use of relay feedback systems to model biological oscillations is a link between classical control theory and biological models. The relay feedback model of gene dynamics explicitly models the logic of a gene turning off/on, and gives new insight into these oscillations. This framework gives us a methodology to approach high-dimensional models, such as the 10 dimensional model for circadian oscillations in *Drosophila* [7].

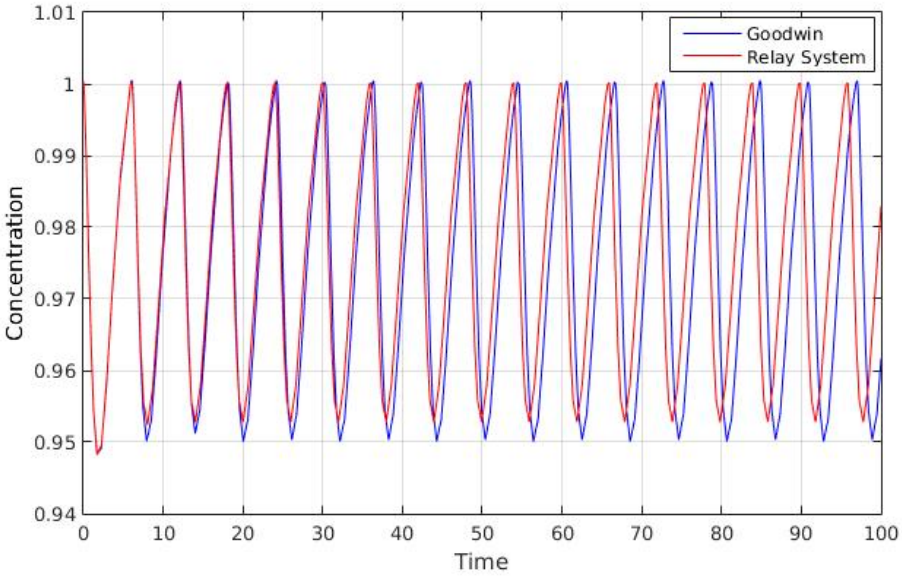

Figure 8: Relay system models Goodwin oscillator well as $p \to \infty$.

3.2 FitzHugh-Nagumo model

In this section, the use of relay feedback systems is extended to model a system where the relay is not as 'obvious', as was in the previous section.

3.2.1 Introduction

The Hodgkin-Huxley model[8] was the first quantitative model of the propagation of an electrical signal along a squid giant axon [6]. It is considered as one of the most important mathematical models in all of the physiological literature [6], and led to the study of excitable systems. The FitzHugh-Nagumo model simplifies the Hodgkin-Huxley model (of four variables) in terms of two variables, one fast and one slow. The FitzHugh-Nagumo model exhibits as clearly as possible the basic dynamic interrelationships between the variables of state which are responsible for the properties of threshold, refractoriness, and finite and infinite trains of impulses [9]. With the fast variable, v, representing the

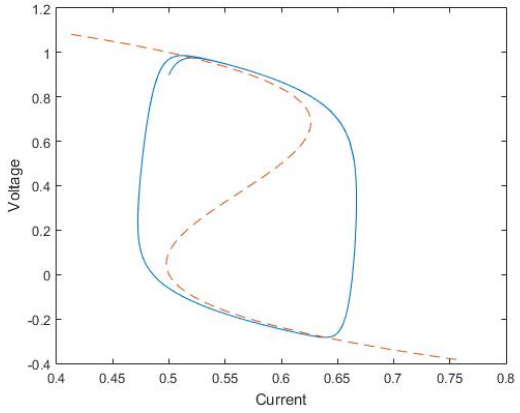

(a) Phase portrait. The cubic nullcline is shown as the dashed line.

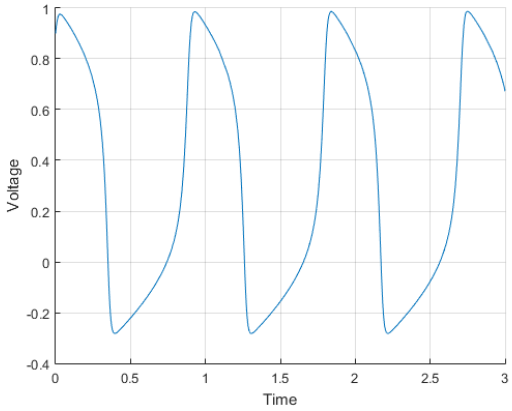

(b) Voltage oscillations.

Figure 9: Continuous oscillations in the FitzHugh-Nagumo model.

voltage and the slow variable, w, representing the current, the FitzHugh-Nagumo model is:

$$\epsilon \dot{v} = f(v) - w + I_{\text{app}} \tag{13}$$

$$\dot{w} = v - \gamma w \tag{14}$$

where:

$$\epsilon \ll 1 \text{ and } f(v) = v(1-v)(v-\alpha)\ , 0 < \alpha < 1.$$

I_{app} is the externally applied current (representing the stimulus). The nullclines[1] of the fast and slow variables have a cubic shape and a linear shape respectively. The input current, I_{app}, shifts the cubic nullcline, affecting where the nullclines intersect, i.e the equilibrium points. For certain input currents, the nullclines intersect at only one (unstable) point and cause continuous oscillations. With $\alpha = 0.1, \gamma = 0.5, \epsilon = 0.01$ and $I_{\text{app}} = 0.5$, the unique rest point is unstable. Since $\epsilon \ll 1$, the fast variable tries to follow the stable branches of the cubic nullcline where possible and then quickly jumps to the other stable branch. That is the voltage stays at a high value for some time and then quickly jumps to a low value and then jumps up to a high value (see Figure 9). Meanwhile, the current slowly adapts to the high/low value of the voltage, pushing the system to leave the stable branches eventually. The behaviour of the system in the phase plane follows from singular perturbation theory[6].

3.2.2 Converting to relay feedback model

As $\epsilon \to 0$, the phase portrait of the voltage and current becomes increasingly 'linear' and closely resembles a skewed relay with hysteresis (Figure 10). This can be understood as high gain inversion [10], and the voltage behaves like the output of a skewed relay. So, when the system is continuously oscillating, it allows us to replace the cubic nullcline with a skewed relay (see Figure 11b).

[1]The nullcline is the line along which a variable's time derivative is zero

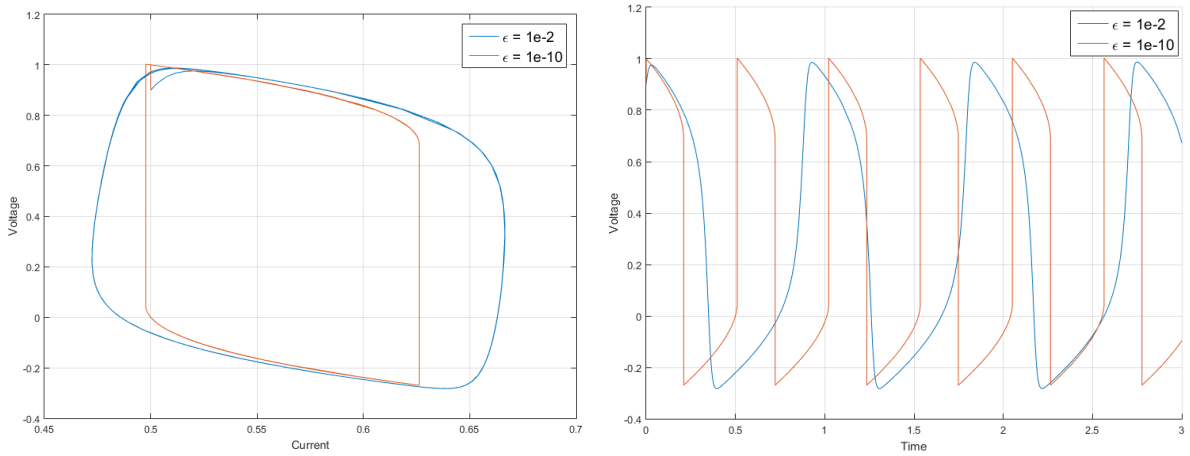

(a) Phase portrait. Hysteresis becomes more 'linear' and 'relay-like'.

(b) Voltage oscillations become more 'discrete', similar to a relay output.

Figure 10: In the limit $\epsilon \to 0$, the voltage output looks like the output of a relay. The hysteresis looks like a skewed relay.

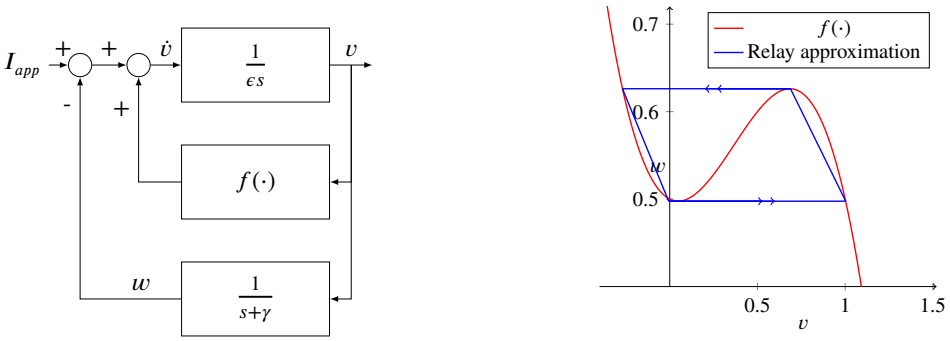

(a) Block diagram

(b) Nonlinearity and the "relay" approximation

Figure 11: FitzHugh-Nagumo model.

High gain inversion:-

$$\epsilon \to 0 \Rightarrow 0 = f(v) - w + I_{\text{app}} \tag{15}$$

$$v = f^{-1}\left(w - I_{\text{app}}\right) \tag{16}$$

$$v \approx \text{Relay}(w) \tag{17}$$

This allows us to replace the inner loop in 11a. With a shift in coordinates to make the 'relay' symmetric about the origin, and a change of basis so that an unskewed relay can be used, results in the relay feedback system in Figure 12. Details of this transformation are illustrated in the Appendix. Now, using equation (3), we can derive the time period of the oscillation and its local stability. The results are shown in Figure 13. The relay feedback model matches the oscillations very closely.

This model reveals how the oscillations can be understood as adaptation around a hysteresis. The current slowly adapts to each switch in voltage, around the relay hysteresis, causing the voltage to oscillate.

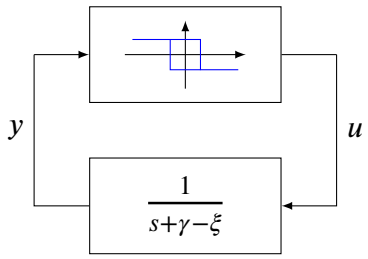

Figure 12: Relay feedback model of FitzHugh-Nagumo.

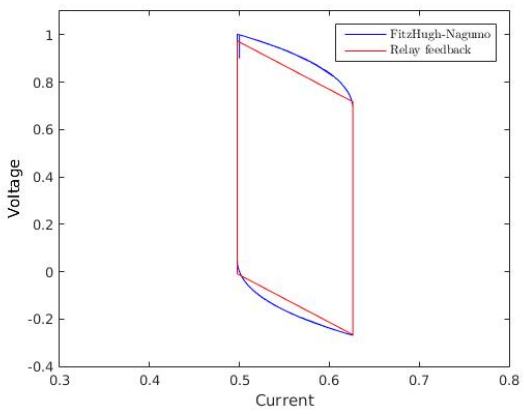

(a) Phase Portrait. Voltage is like the output of a skewed relay.

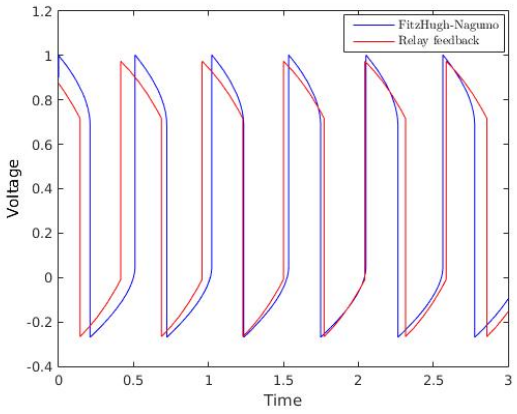

(b) Voltage oscillations against time. Voltage alternates between a high state and a low state.

Figure 13: FitzHugh-Nagumo model and Relay feedback model match in $\lim_{\epsilon \to 0}$

4 Relay feedback model of nested oscillations

In the previous section, the use of the relay feedback framework for analysing simple oscillations was found to be very useful. Now the question arises as to whether this framework is capable of tackling complex oscillations. Bursting, a complex oscillation, can be understood as the interaction between two excitable systems with different time scales[14]. In other words, it can be understood as two coupled FitzHugh-Nagumo models.

In this section, the use of relay feedback analysis is extended to bursting. Following how [13] split bursting into two subsystems, we dissect a bursting normal form into two coupled relay feedback systems.

4.1 Bursting

Bursting is an important signaling component of neurons, characterized by a periodic alternation of bursts (periods of rapid oscillatory activity) and quiescent (membrane potential changes slowly) periods [12]. Bursting observed in cells can have a wide variety of periods, ranging from a few seconds to a few minutes [6]. This general phenomenon is believed to play an important role in several signalling mechanisms. Bursting can also be viewed as a two variable automaton in frequency [14]; encoding

memory into four states– resting, fast oscillations, slow oscillations and bursting.

All neuronal bursters have three distinct time scales: a fast time-scale for spike generation, a slow time-scale for the intra burst spike frequency, and an ultra slow time-scale for the inter burst frequency [12]. The bursting property can be understood in terms of a few canonical positive and negative feedback motifs localized in distinct time scales [14], as shown in Figure 14.

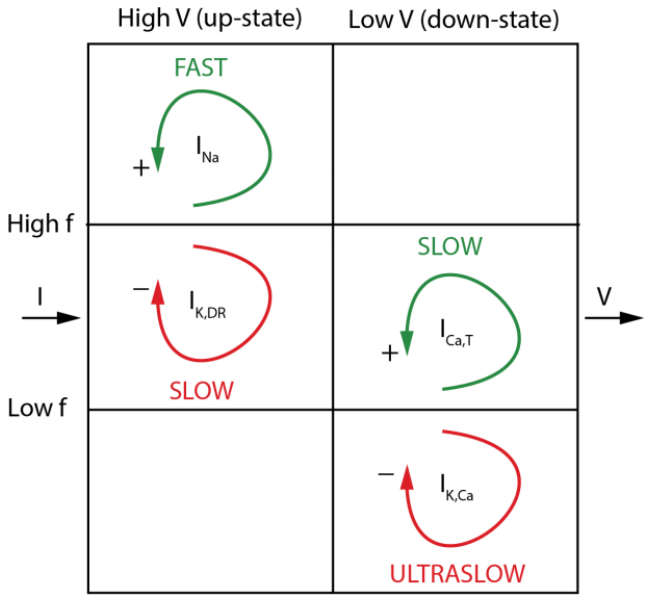

Figure 14: Scheme of the four-state automaton showing the different feedbacks and their localization in frequency (from top to bottom) and in range (from left to right). Green arrows represent positive feedbacks and red arrows represent negative feedbacks. Ionic currents repsonsible for the described feedbacks are noted inside the respective arrows. Source [14].

This separation of timescales is used to decompose bursting into two coupled relay feedback systems. As a first step, a bursting model normal form from [11] is introduced. Then we will step through each of the positive and negative feedbacks, starting at the shortest timescale, and examine how to transform this into relay feedback. Then, the nonlinearities will be simplified to reduce the model into relay feedback systems.

4.2 A three-time scale bursting normal form

The three-time scale bursting normal form organized by the winged cusp singularity is presented in [11]. It is based on unfolding the organizing center called the winged cusp to obtain a finite family distinct, robust static behaviours [11]. The model is based on Singularity theory and the interested reader is referred to [11] for a comprehensive exposition of how this model realises a variety of nonlinear behaviours.

A key feature of this model is the robust coexistence of a stable fixed point and a stable relaxation limit cycle as shown in Figure 15. That is, the model is rest-spike bistable. When spiking, the stable limit cycle is similar to the FitzHugh-Nagumo model's phase portrait. This model generalizes FitzHugh-Nagumo by adding a third variable (ultra-slow) in negative feedback, which adapts in the

dimension normal to the phase portrait (see Figure 16). The basic idea is that there are slow processes which modulate the faster spike generating dynamics [13]. The ultra-slow adaptation switches the behaviour between spiking and resting. The state-space equations for this model are:

$$\begin{aligned} \epsilon_f \dot{x}_f &= -x_f + S\left(x_f + B_\delta\left(u + x_s + \tfrac{\gamma}{2}x_f\right) + \beta x_f + \alpha - x_{us}\right) \\ \dot{x}_s &= x_f - x_s \\ \dot{x}_{us} &= \epsilon_u\left(-x_{us} + k_u(x_f + \bar{x}_u)\right) \end{aligned} \tag{18}$$

where:

$$\begin{aligned} &\text{Sigmoid nonlinearity: } S(u) = \tanh(u) \\ &\text{Bump nonlinearity: } B_\delta(u) := S(u+\delta) - S(u-\delta) - 2S(\delta), \quad \delta \neq 0 \end{aligned} \tag{19}$$

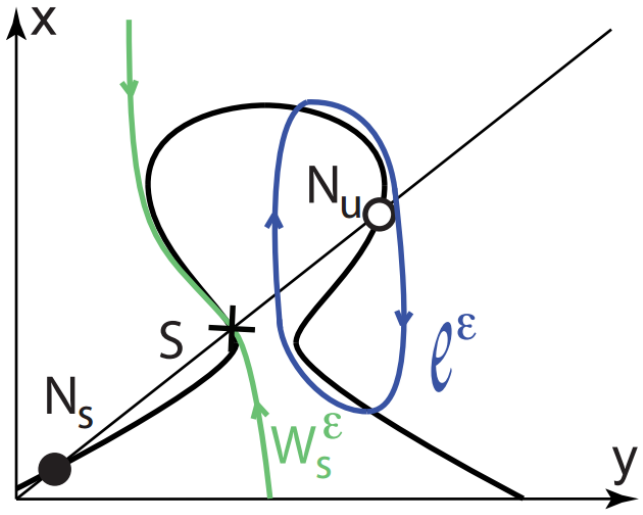

Figure 15: Phase portrait (qualitative) of the three-time scale bursting normal form. N_s is the stable equilibrium, N_u is the unstable equilibrium, S is the saddle point, W_s^ϵ is the stable manifold of S and l^ϵ is a stable limit cycle. The thick black line is the fast variable's nullcline, known as the mirrored hysteresis (winged cusp singularity) and the slow variable's nullcline is the thin straight line. Source [12].

The block diagram for this circuit is shown in Figure 17. Typical bursting is shown in Figure 18.

4.2.1 The fast positive feedback

The fast positive feedback in Figure 17 is the feedback of $H_f(s)$ through the gain $\tilde{\beta}$ and the sigmoid nonlinearity. The fast positive feedback creates a nonlinearity with hysteresis. This can be understood by considering positive feedback for a saturation function, shown in Figure 19. By assuming that x_f is much faster than the other variables, we can replace the positive feedback loop as a relay. This is equivalent to $\epsilon_f \to 0$, which was done earlier for the FitzHugh-Nagumo model.

4.2.2 The slow negative and slow positive feedback

In the slow timescale, there is a mixture of positive and negative feedbacks. This balance of feedback provides a closed-loop behaviour that is either a regulator or a switch [14]. In the normal form, it

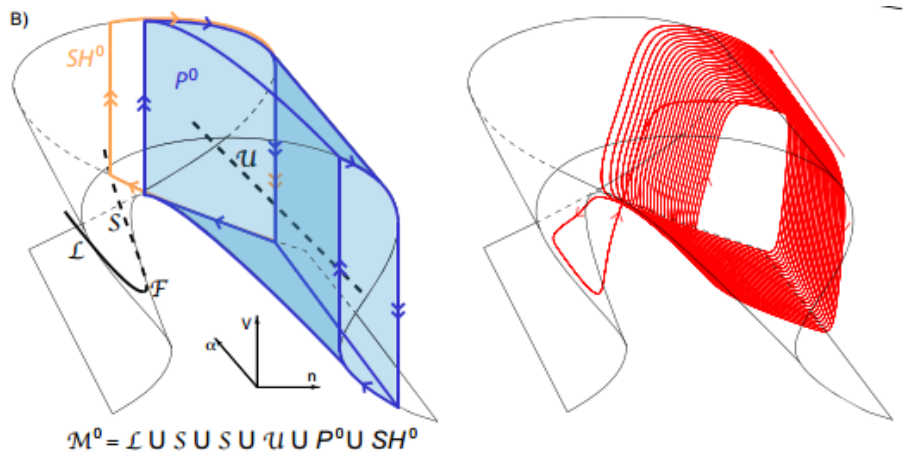

Figure 16: Three-dimensional singular invariant set $\mathcal{M}^0$ (left), which provides a skeleton for a three-time scale bursting attractor (right). The ultra-slow parameter adapts to switch the system from spiking to resting and vice versa. See [12] Figure 4 for details. Source [12].

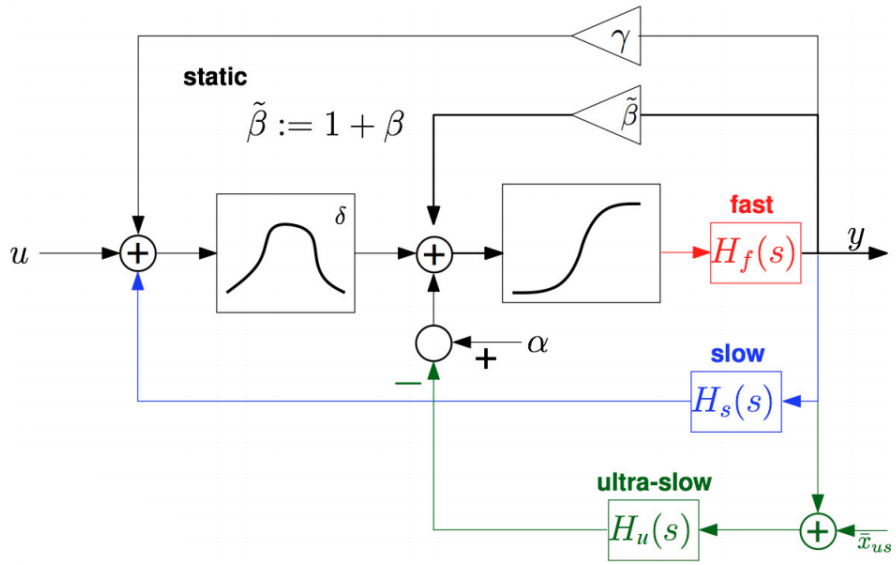

Figure 17: Three-time scale bursting normal form block diagram. Source [11].

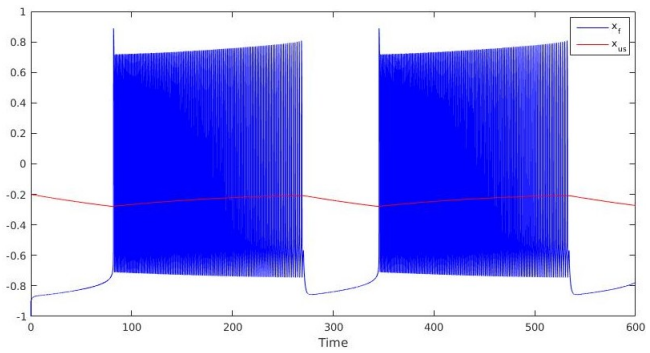

Figure 18: Bursting. The ultra-slow oscillations of the x_{us} switches the output x_f between spiking and resting.

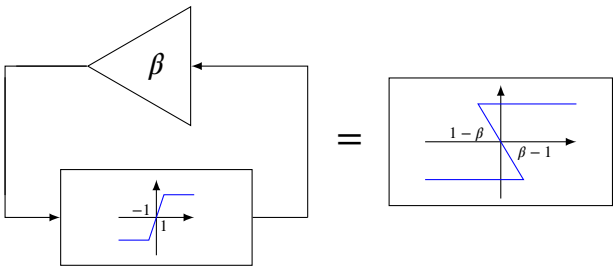

$$y = \begin{cases} 1 \text{ if } x \geq 1 - \beta \\ -1 \text{ if } x \leq \beta - 1 \end{cases}$$

Figure 19: For the saturation function, for $\beta > 1$, the nonlinearity gains a hysteresis of width 2β.

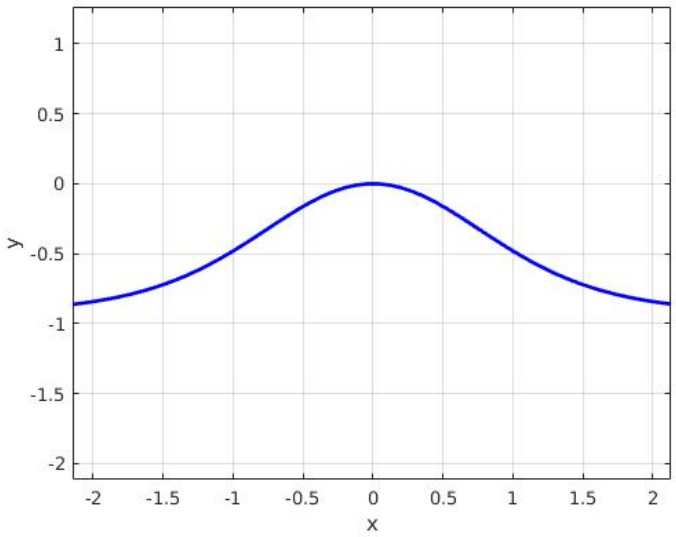

Figure 20: Bump nonlinearity

is the bump nonlinearity (Figure 20) that plays this role and affects what kind of feedback the slow plant provides. For rest-spike bistability, the stable equilibrium is required to be in the region where the slow feedback is positive,i.e the equilibrium is in the regenerative region. This is achieved in the model by having the stable equilibrium in the region where x_s is negative, and the system operates in the region where the bump has a positive gradient. When the system is spiking, the input to the bump is always greater than zero. The bump provides negative feedback in this region, causing the slow plant to adapt around the hysteresis of the sigmoid nonlinearity. That is, when spiking, the model essentially simplifies down to the FitzHugh-Nagumo model during continuous oscillations.

4.2.3 The ultra-slow negative feedback

In the ultra-slow time scale, the H_u provides negative feedback. To understand how this affects the nullcline of the fast variable, the (unfolding) parameter α (see Figure 17) should be examined. The parameter α modulates monotonically the winged-cusp singularity [11], as shown in Figure 21. Consequently, as x_{us} reaches a particular value (its maximum value), the nullclines of the fast and slow variables will only intersect at the stable fixed point (low x_f). This drives the system to the quiescent period, while x_{us} slowly recovers. When x_{us} reaches its minimum value, the nullclines of the fast and slow variables will only intersect at a high x_s which then becomes the unstable fixed point as x_{us} re-

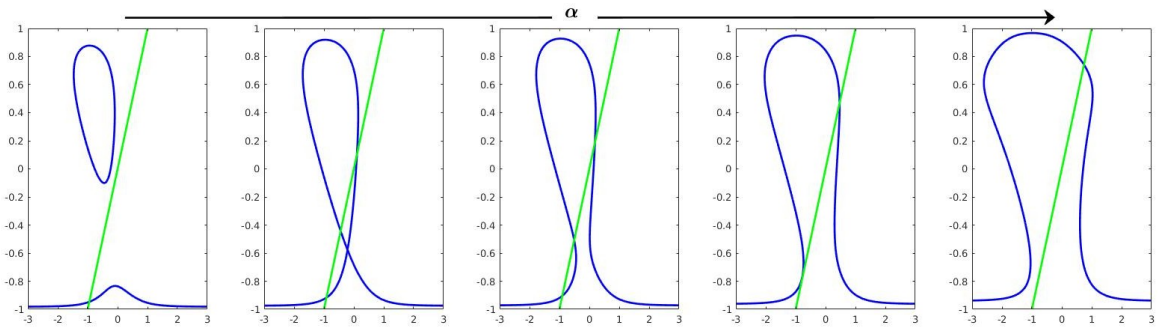

Figure 21: Fast nullcline changing as α increases. Within a fixed range of α, the system has both the resting and the spiking equilibrium. This is the bistable range.

covers. This drives the system to the spiking period. The bursting model thus relies on continuously adapting this parameter, using the ultra-slow variable, around the bistable range (minimum and maximum value of x_{us}). It is clear now that the ultra-slow parameter can be modelled as a relay feedback system, oscillating around the bistable range.

4.2.4 Using piecewise linear nonlinearities

Using linear approximations of the nonlinearities allow us to simplify them to linear gains. As shown in Figure 22, the saturation function is a good approximation to the sigmoidal nonlinearity. Furthermore, since the positive feedback gain is $\tilde{\beta} := 1 + \beta$, this can be replaced by a positive feedback of just β around a relay with no hysteresis (equivalent to the sign$(\cdot)$ function). This is then equivalent to a relay with hysteresis limits $\pm\beta$.

The bump nonlinearity (with δ set to 0.5) can be approximated by the piecewise linear function shown in Figure 23. The piecewise linear function simplifies the model very nicely since the positive/negative feedback gain is constant. The piecewise linear function is:

$$B_p := \begin{cases} \frac{1}{2}x & \text{if } -2 < x < 0 \\ -\frac{1}{2}x & \text{if } 0 < x < 2 \\ -1 & \text{otherwise} \end{cases} \tag{20}$$

The system is now:

$$\begin{aligned} \epsilon_f \dot{x}_f &= -x_f + \text{sign}\left(B_p\left(u + x_s + \tfrac{\gamma}{2}x_f\right) + \beta x_f + \alpha - x_{us}\right) \\ \dot{x}_s &= x_f - x_s \\ \dot{x}_{us} &= \epsilon_u\left(-x_{us} + k_u(x_f + \bar{x}_u)\right) \end{aligned} \tag{21}$$

The system's phase portrait is shown in Figure 24. The new fast nullcline approximates the original nullcline well.

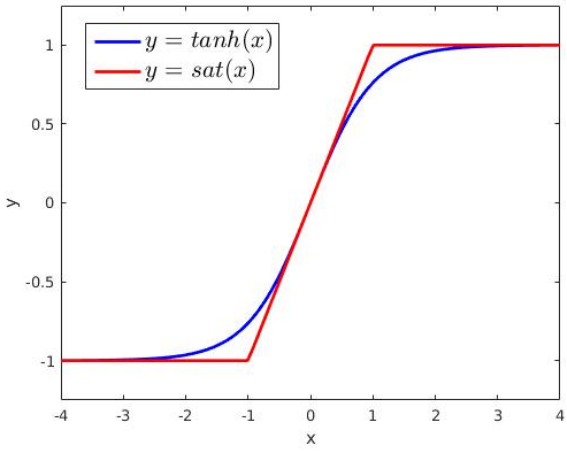

Figure 22: The $S(\cdot)$ and the saturation functions. The saturation function is a good approximation to the $S(\cdot)$.

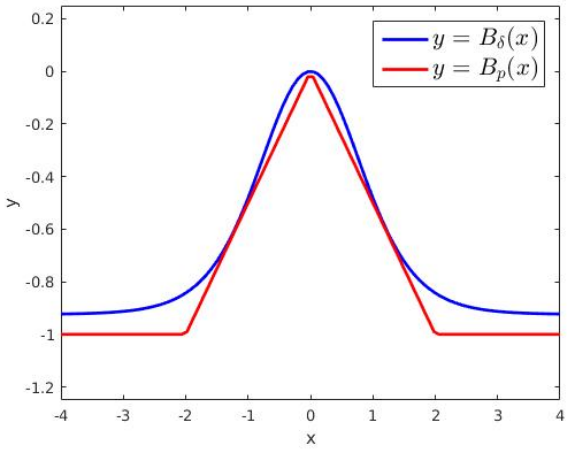

Figure 23: The $B_\delta(\cdot)$ with $\delta = 0.5$ and a piecewise linear approximation $B_p(\cdot)$.

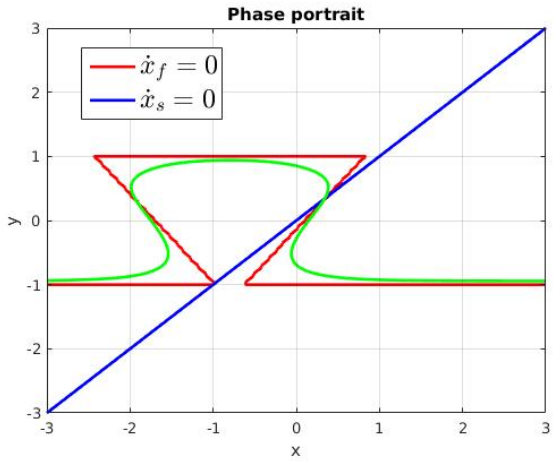

Figure 24: Phase portrait using piecewise-linear nonlinearities. The original fast nullcline is plotted in green for comparison. Note that the lines showing $\dot{x}_f = 0$ where $-1 < x_f < 1$ does not exist algebraically. Numerical computing leads to those lines.

4.2.5 Separation of time scales to separate into relay feedback systems

By assuming that the fast variable changes instantaneously ($e_f \to 0$), the innermost loop involving the fast plant H_f can be replaced by a relay with hysteresis (Figure 25).

While the system is spiking, the bump nonlinearity can be replaced by a constant gain providing negative feedback. Furthermore, Figure 26 shows how the ultra slow variable can be viewed as nearly constant. This is equivalent to the relay feedback system with a slowly shifting hysteresis (Figure 27).

Setting $\gamma = 0$ (without loss of generality), gives a hysteresis for the new system that is not skewed (transformation for skewed hysteresis was carried out in Section 3.2.2). This is now a simple relay feedback system to model the spiking. Using the analytical results from [5] we can now predict the time periods of the fast oscillations. The shifting of the hysteresis limits, due to the ultra slow variable, simply change the time periods of the oscillations as shown in Figure 28.

The ultra-slow variable, due to its slow time constant, can be regarded as only responding to an "averaged" x_f. Figures 29 and 30 reveal the response of α to a moving average x_f. The relay hysteresis limit is the bistable range of α, while the maximum output of the relay is slowly changing as the "averaged" x_f varies as predicted from equation (5). This reveals how the bursting circuit has been simplified into two coupled oscillators. The fast-slow oscillator reproduces the spiking and the average-fast–ultra-slow oscillator dictates when the model spikes and rests (see Figure 31).

The transforming of the bursting model's normal form into relay feedback models enables us to analytically extract the time period of the ultra-slow oscillation and that of the fast oscillation. It also reveals how the two oscillators are linked and how the duty cycle during spiking subtly changes due to the ultra-slow parameter.

Furthermore, this is a step towards multirate feedback systems. [16] developed a theory where an arbitrary multirate sampled system can be replaced by a system with a single-rate sampled system with advance and delay elements. This theory could be amenable to the study of multiple interconnected relay feedback systems, modelling complex biological oscillations.

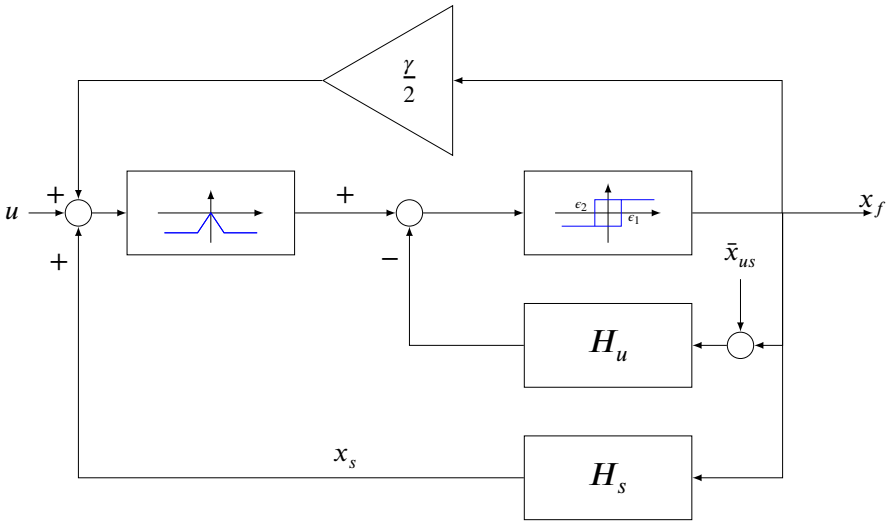

Figure 25: Inner loop replaced by relay with hysteresis. The hysteresis limits are $\epsilon_1 = \beta$ and $\epsilon_2 = \beta$.

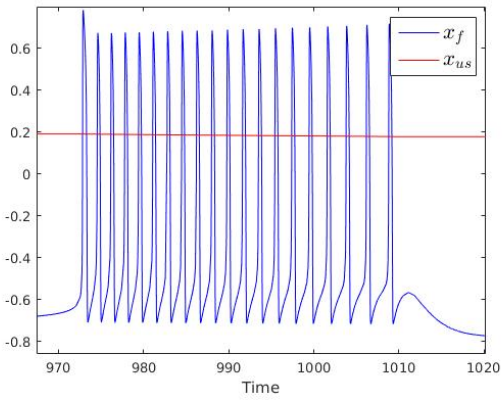

(a) The ultra-slow variable (x_{us}) is almost constant relative to the fast variable (x_f) when spiking.

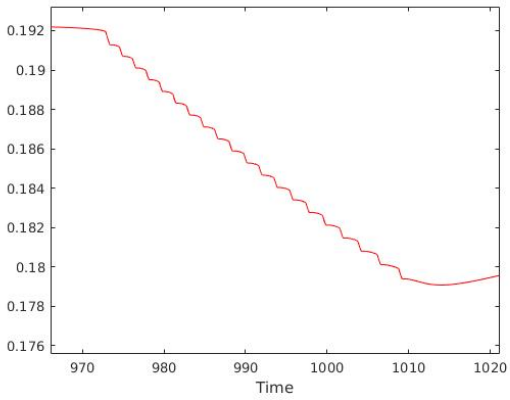

(b) The ultra slow variable's slow change is later found to slowly shift the hysteresis limits of the fast relay to the left during spiking.

Figure 26: Variables changing during a very short period of spiking. The ultra-variable adapts very slowly to the changing shape of the fast variable.

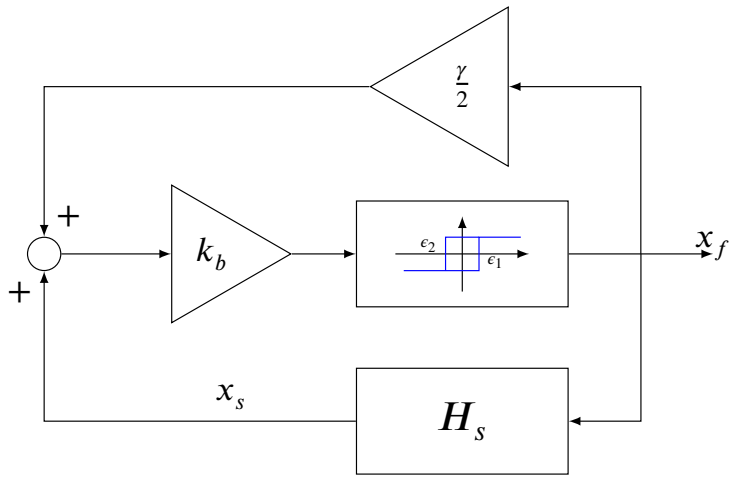

Figure 27: Relay feedback system with slowly shifting hysteresis.$\epsilon_1 = \beta - \alpha - k_b u$ and $\epsilon_2 = -\beta - \alpha - k_b u$

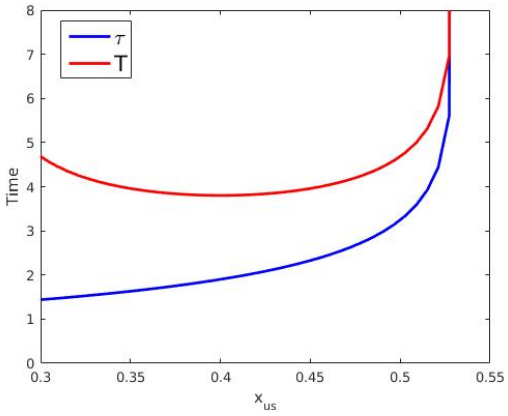

(a) τ falls as x_{us} falls, predicting the duty cycle to become 'balanced' during a burst.

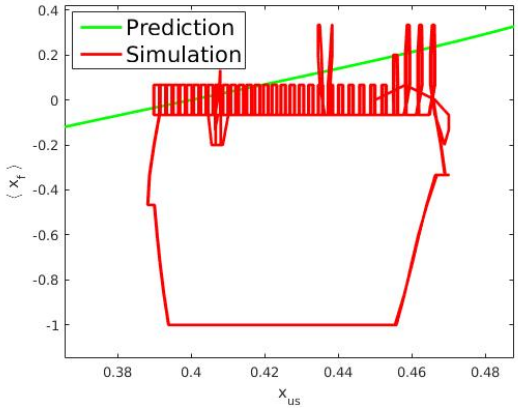

(b) Averaging the time spent in the high and low states (T and τ), gives a prediction of the relay of the ultra slow system. This matches simulation well.

Figure 28: Prediction of the duty cycle of the fast oscillations and of the relay shape of the average-fast–ultra-slow relay feedback system.

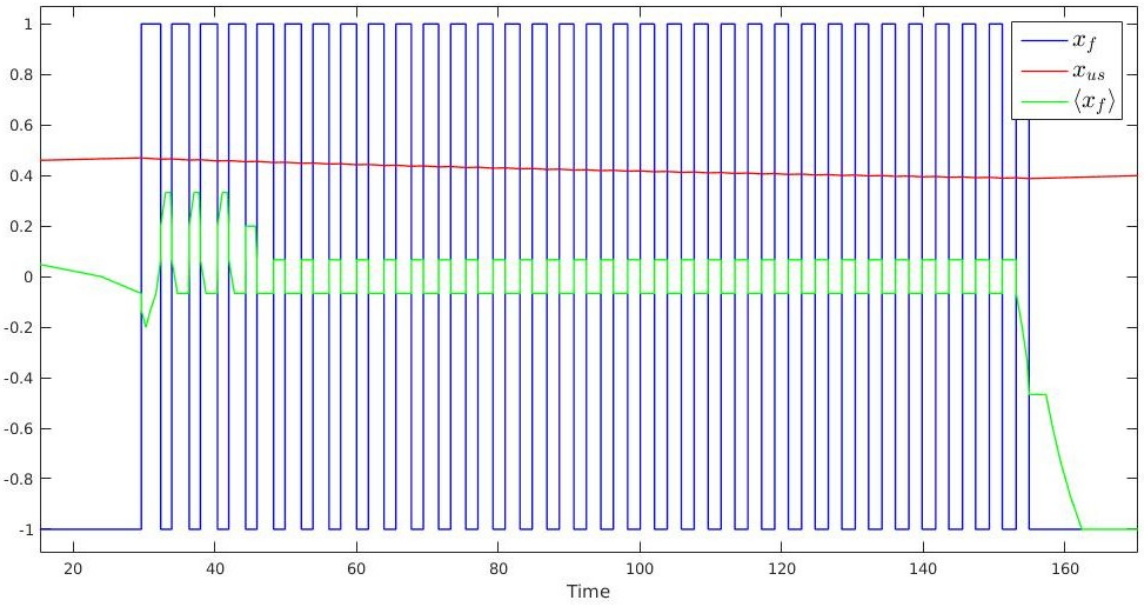

Figure 29: Moving average of x_f changes during spiking as x_{us} changes the hysteresis limits. The effect of the shifting hysteresis is seen as the slowly changing duty cycle of the fast oscillations. The x_f spends a decreasing proportion of time in the high state as the hysteresis shifts lefts. Consequently, the (moving) average, $\langle x_f \rangle$, falls slowly during a burst.

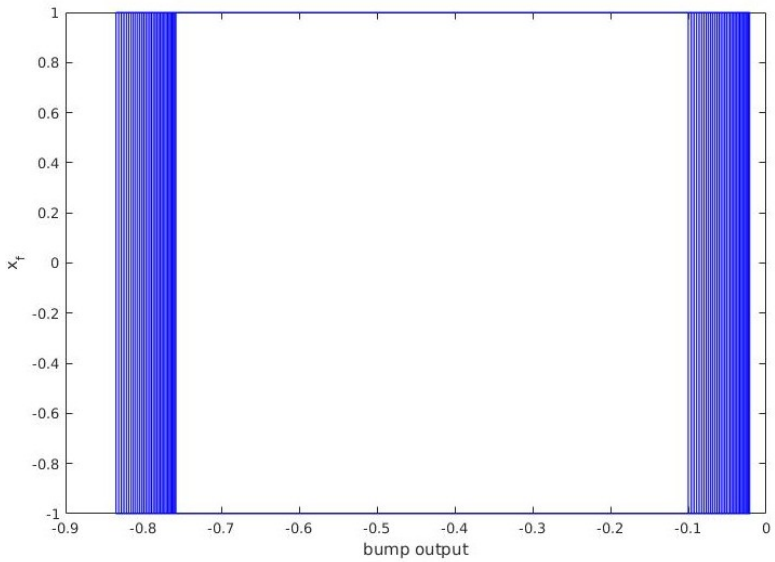

(a) During a burst, the output of the bump nonlinearity slowly shifts to the left. This reveals how the ultra-slow variable essentially shifts the relay hysteresis limits of the fast-slow system during spiking.

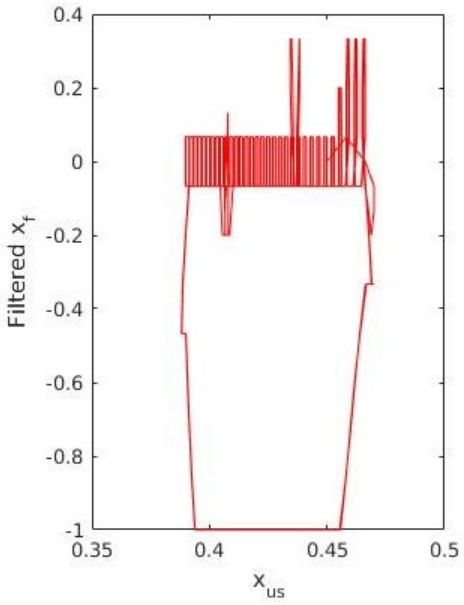

(b) The phase portrait of the (moving) average x_f and the x_{us}. It reveals a relay like hysteresis. The falling $\langle x_f \rangle$ reveals the influence of the fast variable on the relay output magnitude of the ultra slow relay feedback system.

Figure 30: The relay hysteresis of the two relay feedback systems. The fast-slow system has a relay whose hysteresis shift slowly due to the ultra-slow variable. The average-fast–ultra-slow system has a relay whose output magnitude varies as the duty cycle of the fast oscillations change.

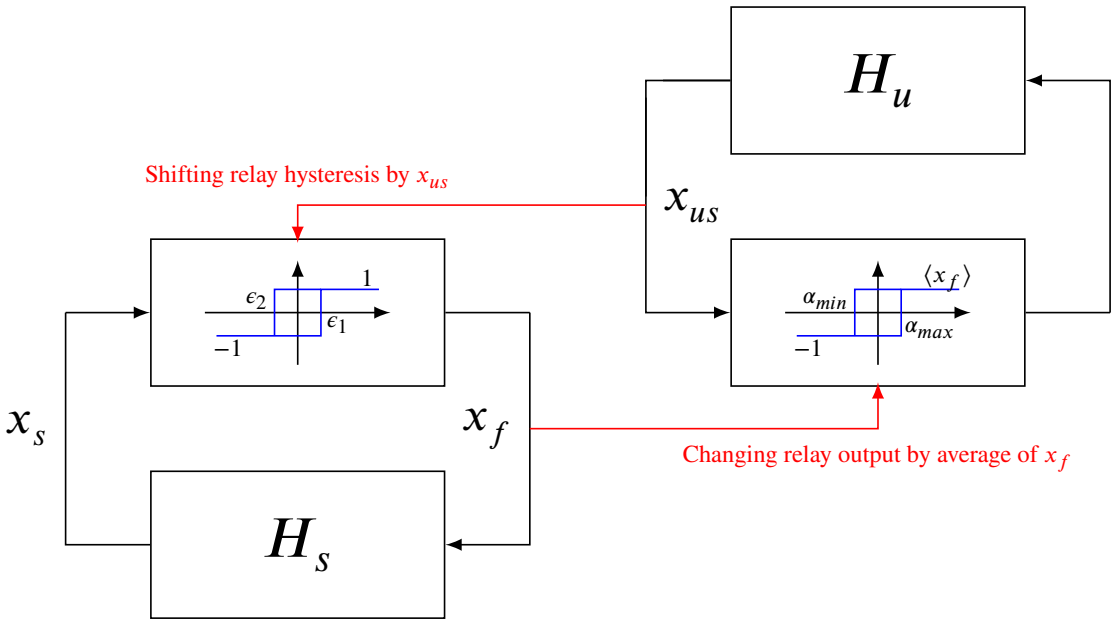

Figure 31: Coupled relay feedback system. The $\langle x_f \rangle$-x_{us} system affects the $x_f - x_s$ system by slowly shifting the hysteresis limits of the relay. The $x_f - x_s$ system affects the $\langle x_f \rangle$-x_{us} system by changing the magnitude of the relay output.

4.3 Hindmarsh-Rose model

The method of breaking down bursting into two coupled relay feedback systems is a general approach. This section proves this by examining how, the Hindmarsh-Rose neuronal bursting model, can be understood as the bursting normal form model and consequently two relay feedback systems.

4.3.1 Introduction

The Hindmarsh-Rose model provides one of the simplest models of the more general phenomenon of oscillatory burst discharge [15]. It is a slight modification of the FitzHugh-Nagumo model for action potentials, with an extra ultra-slow variable. It uses a parabolic nullcline for the slow variable instead of the a straight line and the equations are:

$$\epsilon_f \dot{x}_f = x_s - x_{us} + f(x_f) + I \tag{22}$$

$$\dot{x}_s = g(x_f) - x_s \tag{23}$$

$$\dot{x}_{us} = \tau_{us} \left(k(x_f - \bar{x}_{us}) - x_{us} \right) \tag{24}$$

$$\text{where } f(x) = 3x^2 - x^3 \text{ and } g(x) = 1 - 5x^2.$$

The fast variable, x_f, represents the membrane potential, the slow variable, x_s, is the current and x_{us} is the (ultra-slow) adaptation current. For bursting, the parameters used are $\tau_{us} = 0.001, k = 4, \bar{x}_{us} = 1.6, I = 2$. The behaviour of the model can be seen in Figure 32. The ϵ_f variable has been added to control the speed at which x_f adapts.

The difference between this model and the three time scale bursting normal form model is that the latter places all the nonlinearities in the dynamics of x_f. The Hindmarsh-Rose model mirrors the

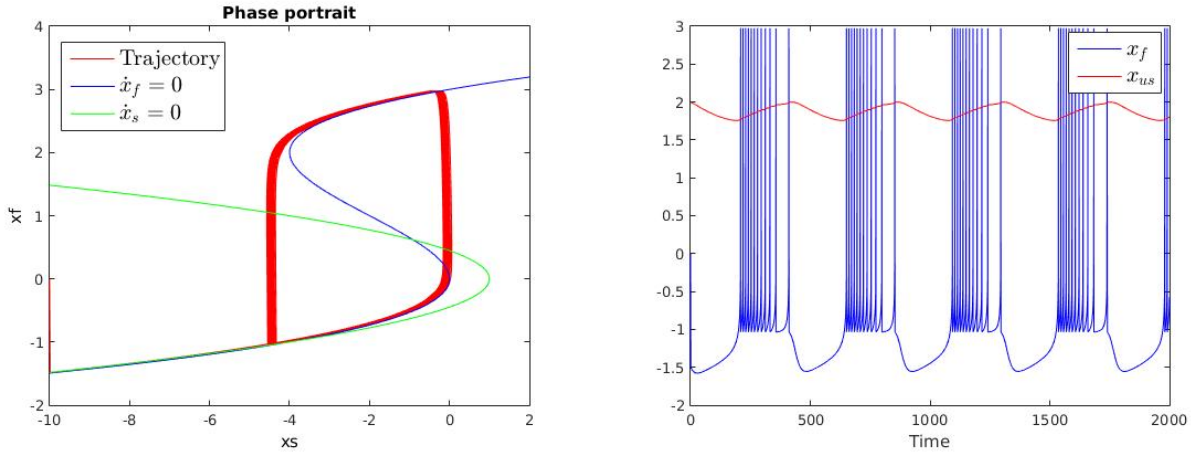

(a) Phase Portrait. Voltage is like the output of a skewed relay as $\epsilon_f \to 0$, just like in the FitzHugh-Nagumo model.

(b) Voltage oscillations against time. Voltage alternates between a high state and a low state when spiking. It then moves to a lower state while resting.

Figure 32: Hindmarsh-Rose model for bursting.

nullcline of x_s by using a quadratic term, while the bursting normal form model mirrors the cubic nullcline using the bump nonlinearity.

4.3.2 Separation of time scales to dissect into relay feedback systems

The Hindmarsh-Rose model has the same key features as the three-time scale bursting normal form (compare the block diagrams in Figure 17 and Figure 34). The fast variable of the Hindmarsh-Rose model is like the output of a relay with shifting hysteresis limits (see Figure 32a) as the ultra-slow variable adapts. Consequently, the fast positive feedback loop of the Hindmarsh-Rose model can be replaced by a skewed relay.

Regarding the slow positive-negative feedback, we need to examine Figure 32. During spiking, the average of x_f is positive and during resting, the average is negative. Since the slow plant is a low pass filter, we can assume that it only responds to the average of x_f. Consequently, similar to the 'bump', for the fast-slow system, the quadratic nonlinearity, $g(x_f)$, provides negative feedback, when spiking and positive feedback when resting.

The ultra-slow negative feedback modulates the shape of the fast nullcline to change the equilibrium positions (see Figure 33) similar to the (unfolding) parameter α of the bursting model normal form. The ultra-slow negative feedback can be again viewed as responding only to the average of the fast oscillations.

Following the same steps as described in the three time scale bursting normal form, the relay feedback model Hindmarsh-Rose model can be constructed. This reveals the capability of the relay feedback framework to addressing models of complex oscillations in literature.

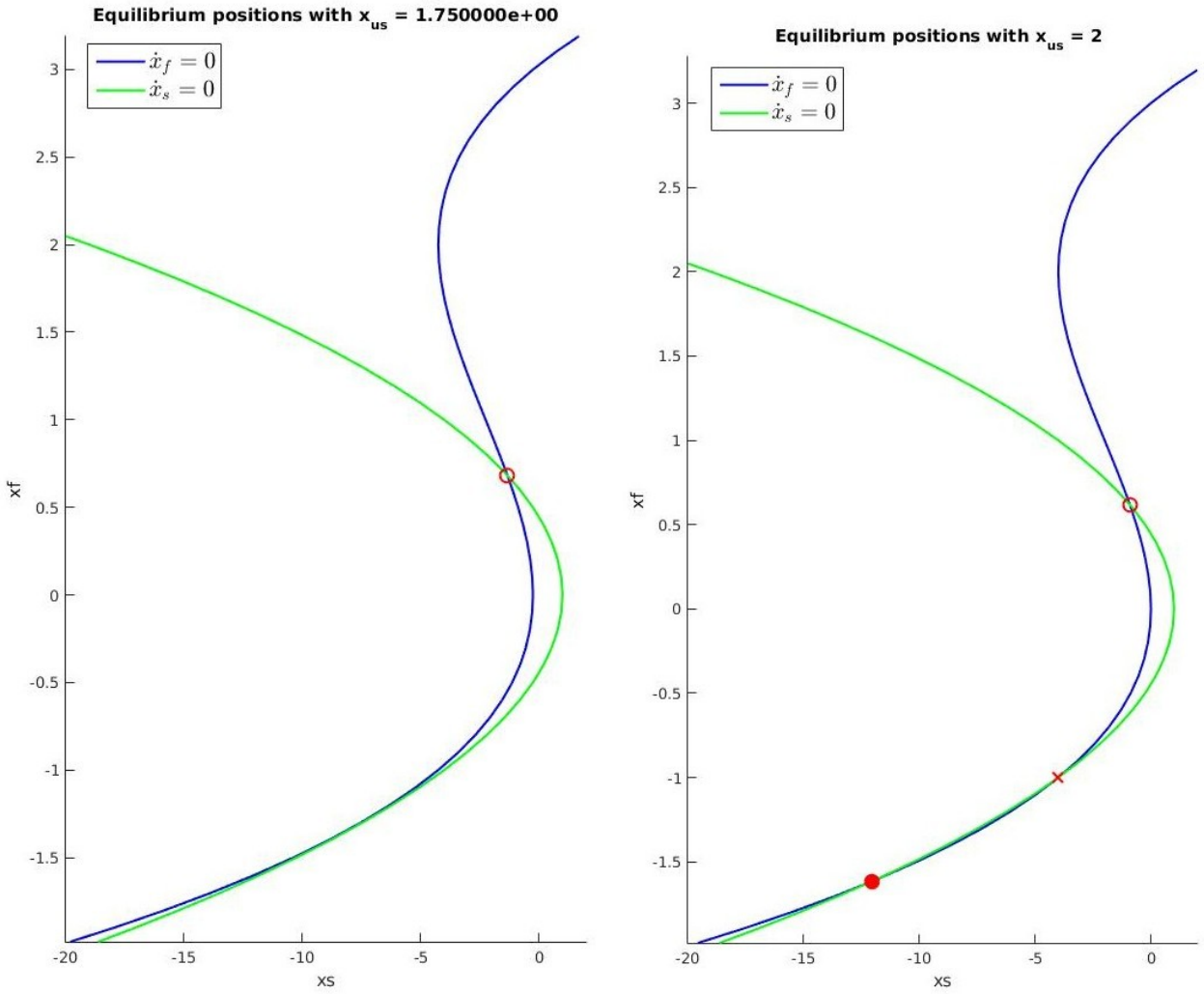

(a) The x_{us} is just small enough that the nullclines intersect only once. The system will switch to spiking as this happens.

(b) The x_{us} is just large enough that the nullclines intersect thrice. The system will switch to resting as this happens.

Figure 33: Fast nullcline of Hindmarsh-Rose model being modulated by the ultra-slow variable (x_{us}). Stable equilibrium is the filled circle, unstable equilibrium is the hollow circle and the saddle point is the cross. Between this range of x_{us}, the system is bistable.

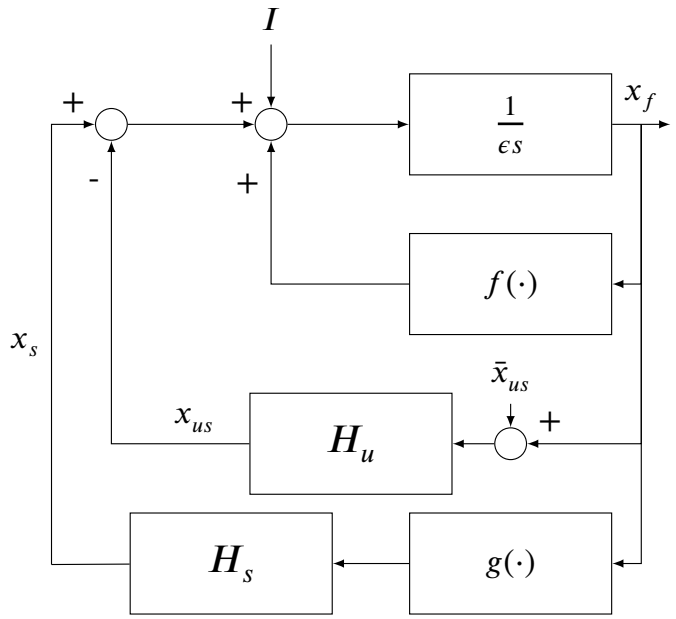

Figure 34: Hindmarsh-Rose model block diagram.

5 Conclusions

The relay feedback framework's capability of modelling biological oscillations was explored. It was shown to be able to model the simple oscillations of the Goodwin and FitzHugh-Nagumo models. It was also shown to be able to simplify a bursting normal form into two coupled relay feedback systems, enabling the Hindmarsh-Rose model to be captured by the relay feedback framework. The relay feedback methodology is appealing since it highlights the interconnection of analogue (L.T.I) systems with digital (relay) logic. Furthermore, it provides analytical tools using which predictions of time periods and stability can found for different parameters. This is a step towards answering the question from [13]: How robust is the bursting mechanism to parameter variations in the physiological range? However, one limitation is that this framework fails to capture the excitatory nature of models. Relay feedback systems are able to capture the oscillatory part of models. Future work in this area would perhaps involve modelling the next level of nested oscillations. Generalizing to an Nth level nested oscillation would provide a link to the theory of multirate feedback systems.

6 Acknowledgements

Prof.Rodolphe Sepulchre is gratefully acknowledged for supervising this project. His insight and guidance throughout the project was invaluable. Thiago Burghi is also gratefully acknowledged for his frequent support and discussions.

References

[1] C.P.Fall, E.S.Marland, J.M.Wagner, J.J.Tyson. (2002). *Computational Cell Biology*. Springer. Volume 20. ISBN 0-387-95369-8.

[2] A.Goldbeter. (2002). *Computational approaches to cellular rhythms.* Nature, Volume 420, Pages 238-245.

[3] A.Goldbeter and M.J.Berridge. (1996). *Biochemical oscillations and cellular rhythms.* Cambridge University Press, ISBN 9780511608193.

[4] C.C.Hang, K.J.Åström, Q.G.Wang. (2002). *Relay feedback auto-tuning of process controllers — a tutorial review.* Journal of Process Control, Volume 12, Pages 143-162.

[5] K.J.Åström. (1995). *Oscillations in systems with relay feedback*. IMA Vol. Math. Appl. : Adap. Control, Filtering, Signal Processing, Volume 74, Pages 1-25.

[6] J.Keener and J.Sneyd. (2009). *Mathematical Physiology*. Springer-Verlag New York. Volume 8/I. Second Edition. ISBN 978-0-387-75846-6.

[7] J.C.Leloup and A.Goldbeter. (1998). *A model for circadian rhythms in Drosophila incorporating the formation of a complex between PER and TIM proteins*. J.Biol.Rhythms, Volume 13, Pages 70-87.

[8] A.Hodgkin and A.Huxley. (1952). *A quantitative description of membrane current and its application to conduction and excitation in nerve.* J. Physiol, Volume 117, Pages 500-544.

[9] R.FitzHugh. (1961). *Impulses and physiological states in theoretical models of nerve membrane*. Biophysical Journal, Volume 1, Pages 445-466.

[10] G.C.Goodwin, S.F.Graebe, M.E.Salgado. (2000). *Control System Design*. Prentice Hall, ISBN 978-0-13-958653-8.

[11] A.Franci and R.Sepulchre. (2014). *Realization of nonlinear behaviours from organizing centers.* Proc. 53st. IEEE Conf. Decision Contr., Pages 56-61.

[12] A.Franci, G.Drion and R.Sepulchre. (2014). *Modeling the modulation of neuronal bursting: a singularity theory approach.* SIAM Journal of Applied Dynamical Systems, Volume 13, Pages 798-829.

[13] J.Rinzel. (1986). *A formal classification of bursting mechanisms in excitable systems.*, Proc. Int. Cong. Mathematicians, Berkeley, California, USA.

[14] G.Drion, T.O'Leary, J.Dethier, A.Franci and R.Sepulchre. (2015) *Neuronal behaviors: a control perspective.* 54th IEEE Conference on Decision and Control, Osaka, Japan, Pages 1923-1944. Tutorial paper.

[15] J.L.Hindmarsh and R.M.Rose. (1984). *A model of neuronal bursting using three coupled first order differential equations*, Proc. R. Soc. Lond., Volume 221, Pages 87-102.

[16] G.M.Kranc. (1957). *Input-output analysis of multirate feedback systems.* IRE Transactions on Automatic Control, Volume 3, Pages 21-28.

Appendices

A Local stability of the relay model of Goodwin oscillator

To check the local stability of the relay model of the Goodwin oscillator, we use Theorem 5.2 from [5]. It requires that the eigenvalues of the W matrix lies within the unit disc. The matrix is defined as:

$$W = \left(I - \frac{w_2 C}{C w_2}\right) \Phi_2 \left(I - \frac{w_1 C}{C w_1}\right) \Phi_1 \tag{25}$$

where

$$w_1 = \Phi_1(Aa_1 + Bd_1) \tag{26}$$
$$w_2 = \Phi_2(Aa_2 - Bd_2) \tag{27}$$
$$a_1 = (I - \Phi)^{-1}(\Phi_2\Gamma_1 d_1 - \Gamma_2 d_2) \tag{28}$$
$$a_2 = (I - \Phi)^{-1}(-\Phi_1\Gamma_2 d_2 + \Gamma_1 d_1) \tag{29}$$
$$\tag{30}$$

and as defined in Section 2.2

$$\begin{aligned} &\Phi = e^{AT}\ ,\ \Phi_1 = e^{A\tau}\ ,\ \Phi_2 = e^{A(T-\tau)} \\ &\Phi_1 = \int_0^{\tau} e^{As} \mathrm{d}s B\ ,\ \Gamma_2 = \int_0^{T-\tau} e^{As} \mathrm{d}s B \end{aligned} \tag{31}$$

For our model, the oscillation is split such that $\tau = 0.19s$ and $T = 5.93s$. With A, B, C defined by equations (10) and (11), we get that:

$$W = 10^{-2} \begin{bmatrix} -2.0 & -3.1 & -8.6 \\ -5.6 & -8.8 & -24.2 \\ 0.0 & 0.0 & 0.0 \end{bmatrix} \tag{32}$$

which has eigenvalues $-7.9 \times 10^{-6}, -1.1 \times 10^{-2}$ and 0. Hence the limit cycle is locally stable.

B FitzHugh-Nagumo to standard relay feedback

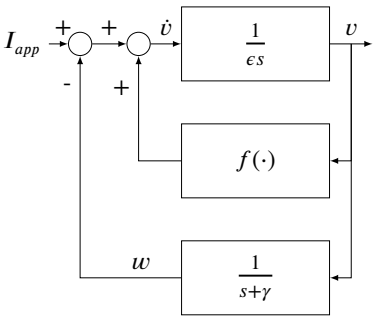

(a) Block diagram

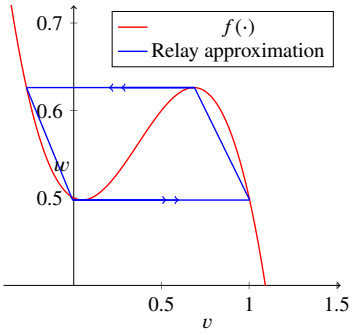

(b) Nonlinearity and the “relay" approximation

Figure A1: FitzHugh-Nagumo

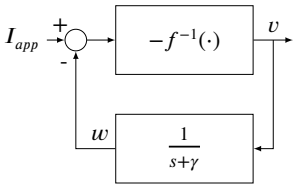

Figure A2: High gain inversion

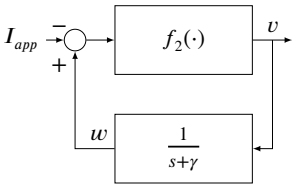

Figure A3: $f_2(x) = -f^{-1}(-x)$

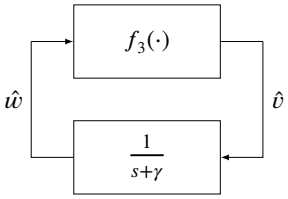

(a) Block diagram

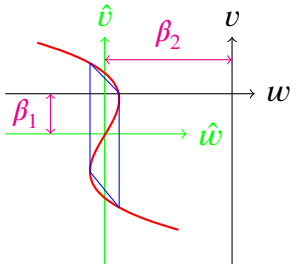

(b) Nonlinearity in new coordinates, $f_3(\cdot)$

Figure A4: Shift coordinate system to make relay symmetric, I_{app} disappears. $\hat{w} = w + \beta_2$ and $\hat{v} = v + \beta_1$

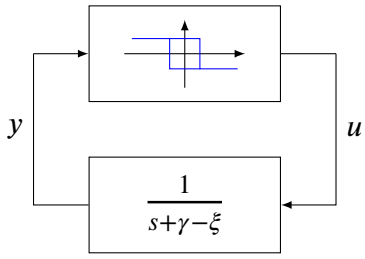

Figure A5: Change of basis to use relay. $\hat{w} = y$ and $\hat{v} = \xi y + u$

Following the steps from the Figures A1 to A5 allow the standard relay to be used to model the FitzHugh-Nagumo equations. The original variables can be recovered as:

$$\begin{cases} v = \hat{v} - \beta_1 = \xi y + u - \beta_1 \\ w = \hat{w} - \beta_2 = y - \beta_2 \end{cases}$$

The first step in replacing the cubic nullcline was to approximate it using a skewed relay. This involved selecting four points on the nullcline that represented the essential behaviour. The points chosen were:

$$(-0.2693, 0.6262), (0.6883, 0.6262), (-0.0061, 0.4976), (1.003, 0.4976) \tag{33}$$

These points now represent the nonlinear function $f(v)$. They undergo the transformations described in the above figures in order to convert them to a standard relay feedback system. To inverse the $f(v)$, each point was reflected about the $y = x$ line. Then they were reflected about the x-axis in order to swap the signs of the input signals. Next, they were reflected in the y-axis due to the minus sign. To centralise the relay about the origin, the points were shifted by $(\beta_2, \beta_1) = (-0.562, -0.354)$. ξ was then chosen in order to get a standard relay — multiply each point by the matrix S,:

$$S = \begin{bmatrix} 1 & 0 \\ -\xi & 1 \end{bmatrix} = \begin{bmatrix} 1 & 0 \\ 2 & 1 \end{bmatrix} \tag{34}$$

This resulted in the four points being positioned at:

$$(0.0643, 0.4917), (0.0643, -0.4917), (-0.0643, 0.4917), (-0.0643, -0.4917) \tag{35}$$

The skew matrix can be understood by considering the skewed relay as simply a relay with an extra loop as shown below. The equations show where the skew matrix comes from. Lumping the extra loop with the original plant gives the new system.

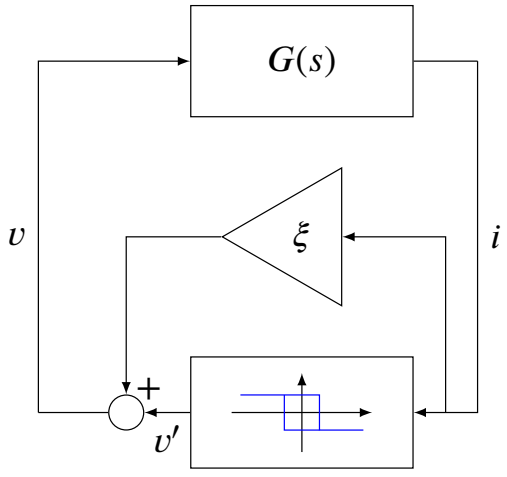

Figure A6: Skewed relay

$$i = G(s)v \tag{36}$$

$$v = \xi i + v' \tag{37}$$

$$\text{we want } i \text{ in terms of } v' \tag{38}$$

$$i = G(s)(\xi i + v') \tag{39}$$

$$i = \left(\frac{G(s)}{1 - \xi G(s)}\right) v' \tag{40}$$

$$G(s) = \frac{1}{s + \gamma} \tag{41}$$

$$\Rightarrow i(s) = \left(\frac{1}{s + \gamma - \xi}\right) v'(s) \tag{42}$$

This is a standard relay with hysteresis limits $\epsilon = 0.0643$ and output $d = 0.4917$. The state-space representation of this system was thus:

$$\dot{x} = (\gamma - \xi)x + u = 2.5x + u \tag{43}$$

$$y = x \tag{44}$$

$$u = \begin{cases} -0.4917 \text{ if } e > 0.0643 \text{ or } (e > -0.0643 \text{ and } u(t-) = 0.4917) \\ 0.4917 \text{ if } e < -0.0643 \text{ or } (e < 0.0643 \text{ and } u(t-) = -0.4917) \end{cases} \tag{45}$$

The original system is then recovered by:

$$v = \xi y + u - \beta_1 = -2y + u + 0.354 \tag{46}$$

$$w = y - \beta_2 = y + 0.562 \tag{47}$$

Using equation (3), the time period was predicted to be 0.54 seconds. The local stability was tested using Theorem 3.1 of [5], with the W matrix being equal to zero and hence having eigenvalues within the unit disk.

C Bursting normal form

C.1 The bistable range in the simplified bursting normal form

In order to find the bistable range for the piecewise linear model of the system, it requires us to find the two critical points at which the system changes from having only one equilibrium to two equilibriums. This was shown for the original model in Figure A7.

The fast nullcline can be written as:

$$G(x_f, x_s, \alpha) = -x_f + \text{sign}\left(B\left(u + x_s + \tfrac{1}{2}\gamma x_f\right) + \beta x_f + \alpha\right) \tag{48}$$

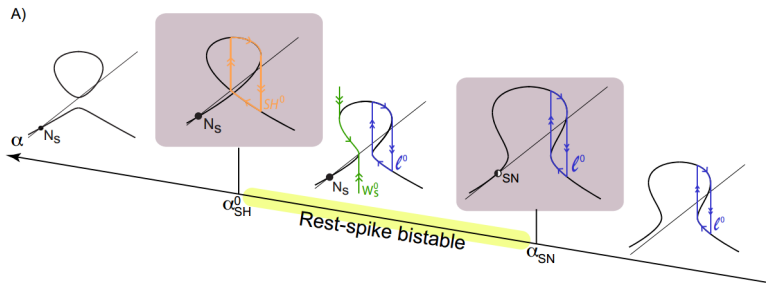

Figure A7: The bistable range for the α parameter.

The extreme point of the lower branches when the sign $(\cdot)$ function changes from being 1 to -1. Since $x_f = -1$, this means: $B(u + x_s - \frac{1}{2}\gamma) - \beta + \alpha = 0$. This can be written as:

$$\tfrac{1}{2}(u + x_s - \tfrac{1}{2}\gamma) - \beta + \alpha = 0 \qquad \text{if } -2 < (u + x_s - \tfrac{1}{2}\gamma) < 0 \tag{49}$$

$$-\tfrac{1}{2}(u + x_s - \tfrac{1}{2}\gamma) - \beta + \alpha = 0 \qquad \text{if } 0 < (u + x_s - \tfrac{1}{2}\gamma) < 2 \tag{50}$$

$$\tag{51}$$

We are first concerned at which point the linear nullcline intersects the lower left hand branch of the fast nullcline. At that point, $x_f = -1$. This implies that $x_s = -1$ as well. This means:

$$\alpha_{max} = \beta + \tfrac{1}{2}(u - 1 - \tfrac{1}{2}\gamma) \tag{52}$$

The two extreme points of the lower branch meet when we reach the peak of the bump, i.e $u + x_s - \frac{1}{2}\gamma = 0$. Thus:

$$\alpha_{min} = \beta \tag{53}$$

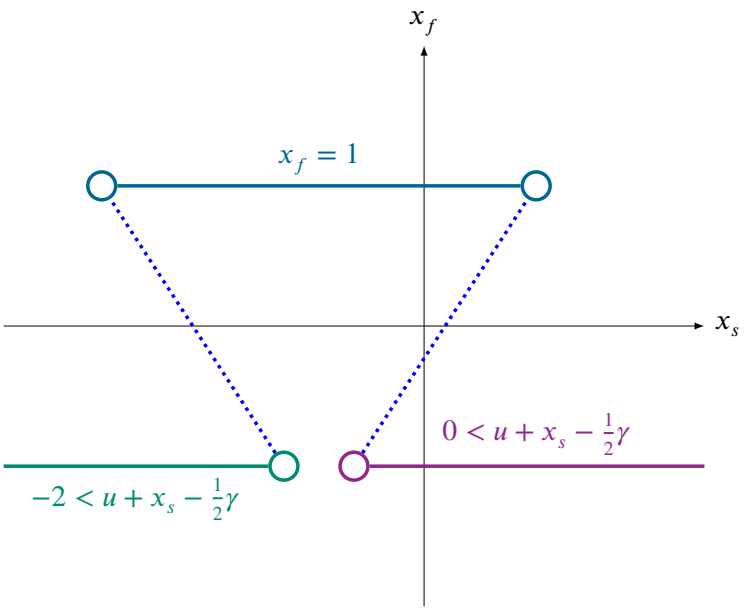

Figure A8: Fast nullcline branches.

C.2 Implementation details

For the bursting normal form model, the parameters used for Figure 26 were: $\alpha = 0.5, \beta = 0.45, \gamma = 1, \delta = 0.5, u = 0.8, k_u = 1, \bar{x}_{us} = 0.5, \epsilon_f = 0.0075$ and $\epsilon_u = 1000$. For the bursting normal form that used piecewise linear nonlinearities, the parameters settings used were: $\alpha = 0.45, \beta = 0.37, \gamma = 0, u = 0.8, \bar{x}_{us} = 0, k_u = 1, \epsilon_f = 0.0075$ and $\epsilon_u = 800$. These were used to produce Figure 29 and 30.

D Risk assessment retrospective

This project was research oriented and involved using MATLAB and Simulink in order to simulate different models. The only risks were those associated with working on a computer for extended periods of time. This was as expected at the onset of the project. Taking regular breaks and good posture helped to reduce the risks.